

Structural characterization of self-organized nanostructures

© S. Ruvimov, Z. Liliental-Weber, J. Washburn, N.N. Ledentsov*, V.M. Ustinov*, V.A. Shchukin*, P.S. Kop'ev*, Zh.I. Alferov*, D. Bimberg**

Lawrence Berkeley National Laboratory, CA94720 Berkeley, USA

* A.F. Ioffe Institute, 194021 St. Petersburg, Russia

** Technische Universität Berlin, D-10623 Berlin, Germany

Self-organized nano-objects fabricated in different semiconductor systems are currently in focus of scientific interest because of their unique electronic properties. Transmission electron microscopy and high resolution electron microscopy have been used to study the InAs quantum dots grown by molecular beam epitaxy (MBE) on GaAs and InP substrates. Optimal imaging conditions for visualization of quantum dots were established. Size, shape and stability of the equilibrium island arrays were analysed with respect to the growth conditions. Both decrease and increase of the As-pressure compared to the optimal value were shown to destroy the regular arrangement of the islands. Energy benefit due to the strain relaxation in the InAs islands is likely to be the driving force for their formation.

Further progress in opto- and microelectronics currently involves quantum effects in semiconductor heterostructures of reduced dimensionality: quantum wires and quantum dots (QDs). Quantum objects uniform in size and in shape can be fabricated in a way compatible with advanced semiconductor technology by utilizing self-organization phenomena during crystal growth [1–12], alloy decomposition [13–15] and surface facetting [16,17]. The Stranski–Krastanow epitaxial growth of highly mismatched, semiconductor systems (Si/Ge [2], InAs/GaAs [4,6,7], GaSb/GaAs [11], ZnSe/ZnS [12], etc) has been shown to result in the formation of coherent strained nm-scale islands that allow attainment of a high level of quantum confinement [4–7]. Vertical coupling of quantum dots in superlattices has been found to decrease the radiative lifetime and to result in injection lasing at low current densities [18]. The understanding of these phenomena is dependent on the employment of atomic level electron microscopic techniques such as high resolution transmission electron microscopy (HREM) [6,7] and scanning tunneling microscopy (STM) [4]. These techniques are complementary: STM is efficient for surface characterization and morphology evaluation during growth while HREM is used to characterize atomic structure of quantum objects. Due to the small sizes of quantum objects and the strain effects, their HREM visualization requires special imaging conditions. Here we review results on structural evaluation of self-organized nano-objects fabricated in different semiconductor systems.

Scattering in size and shape for the quantum dots reported by different groups makes it of interest to study the equilibrium geometry of small islands grown in the Stranski–Krastanow mode. A typical HREM image of an InAs quantum dot is shown in Fig. 1. Pyramid-like InAs islands with 14 nm base length and 7 nm height are embedded in the GaAs active layer which is located between two cladding superlattices of $(2 \text{ nm Al}_{0.3}\text{Ga}_{0.7}\text{As}/2 \text{ nm GaAs})_{10}$. Strain-induced contrast significantly influences the image, but the pyramidal shape of the island is still visible. A plan-view image of this heterostructure (not shown) demonstrates ordering of the islands in both shape and size [7].

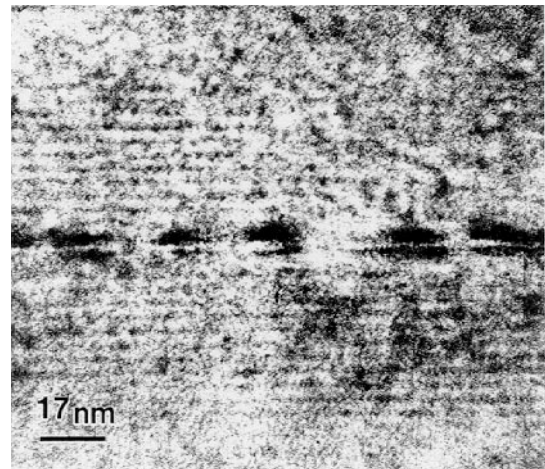


Figure 1. InAs quantum dots in GaAs: HREM cross-section (a) and plan-view (b) TEM micrographs.

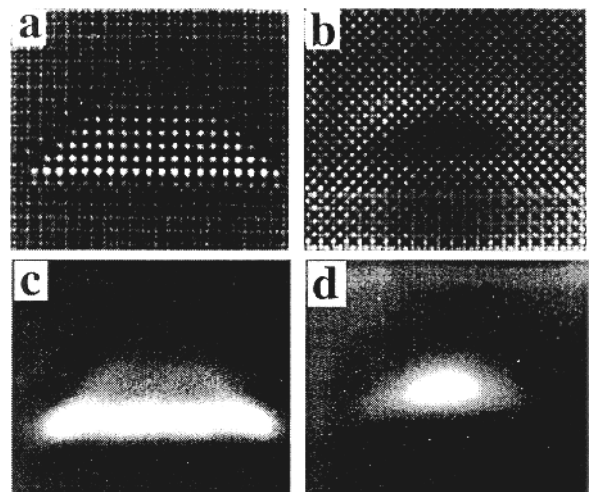


Figure 2. Simulated cross-sectional HREM (a,b) and corresponding bright-field (c,d) images of unrelaxed (a,c) and relaxed (b,d) InAs island.

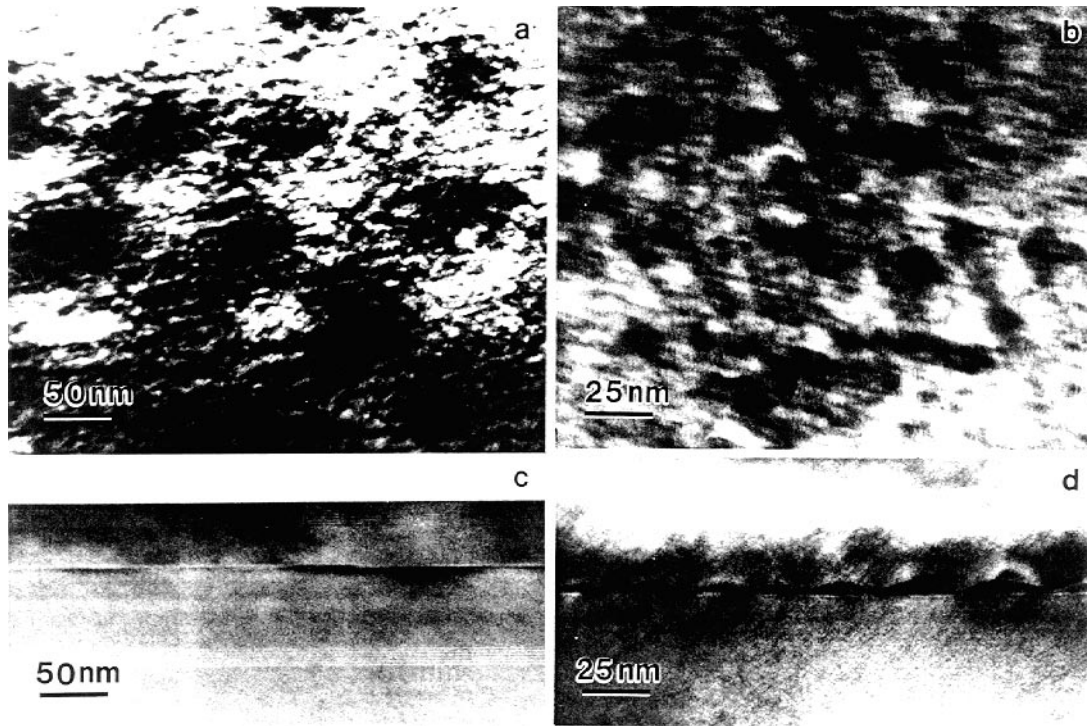


Figure 3. Plan-view (*a,b*) and cross-sectional (*c,d*) bright-field TEM images of InAs dots for InAs/InGaAs (*a,c*) and InAs/InAlAs (*b,d*) systems grown on (001) InP substrates.

Because the strain-induced contrast strongly affects the dot image on TEM micrographs, optimization of imaging conditions is required to visualize the true shape and size of the quantum dot. Molecular dynamics calculations have been applied to model the atomic displacement field of the InAs island and the GaAs matrix. The calculations were carried out using the CERIU program package (Molecular Dynamics Ins., Cambridge) detailed elsewhere [19]. A pyramid-like InAs island has a base length $a = 6$ nm because the total number of atoms in the model was limited to $2 \cdot 10^4$. The atomic displacement field has then been used for simulations of HREM images at different foil thicknesses and defoci [19]. Fig. 2 shows the calculated HREM image and corresponding calculated bright-field images of unrelaxed (*a, c*) and relaxed (*b, d*) InAs islands. An increase of foil thickness significantly affects the image due to strain-induced contrast so that the true size and shape of the island is poorly resolved at foil thickness larger than $2a$. The island contrast is most clearly seen at certain defoci (60–70 nm for JEOL 4000EX microscope), where the chemical contrast difference is most pronounced [19]. Detuning from these optimal imaging conditions results in the over- or underestimation of the QD size. Strain affects conventional TEM image of QDs even more strongly. Contrast on calculated bright-field images taken at symmetrical Laue orientation [e.g. in Fig. 2 (*d*)] depends on the foil thickness, but is independent of defocus. Even for a thin foil, the shape of the dot is difficult to resolve. However, the size of the dot can be

determined if the thickness of the foil is not larger than $2a$. Similar results were found for plan view imaging [19].

Formation of InAs dots on InP substrates differs from that on GaAs and significantly depends on the material of the matrix. Fig. 3 shows typical TEM images for InAs/InGaAs and InAs/InAlAs systems grown on (001) InP substrates. The InGaAs and InAlAs ternary alloys had the same lattice parameters as the InP substrate. The characteristic lateral sizes of InAs quantum dots were 50–70 nm for InAs/InGaAs and InAs/InAlAs systems, respectively. The dot heights were in the range of 2.5–3 nm in both cases. Besides the InAs dots, strain modulation contrast due to spinodal decomposition of ternary alloys was observed along $\langle 110 \rangle$ directions. Similar composition modulations have been reported for other systems [13,14]. The InAs dots in Fig. 3 are more rounded and more shallow for the InAs/InGaAs system compared with that of the InAs/InAlAs.

In contrast, each island in the InAs/GaAs system has a square base and they are locally arranged in a two dimensional square lattice with main axes along $\langle 100 \rangle$ crystallographic directions [6,7]. The square base of the islands can be understood by taking into account the elastic anisotropy of cubic GaAs with the minimum stiffness along $\langle 100 \rangle$ and $\langle 010 \rangle$ crystallographic directions. The repulsive interaction of islands of high density due to the strained substrate results in their ordering into the two dimensional square lattice. The uniform quantum dot array can result in minimal possible free energy of the system [20]. Thus, the characteristic size of the island is energetically favorable.

According to our calculations [20], the total energy of the system has a minimum for a particular dot size which depends on material parameters. This agrees well with observations of the effect of growth interruption and variation in As pressure on dot sizes and their distribution (not shown). Growth interruption for 40 s after 2.5 ML InAs is deposited is enough to let the dot reach the equilibrium size that was typical for 4 ML InAs deposition without growth interruption. Both decrease and increase of the As-pressure compared to the optimal value were shown to destroy the regular arrangement of the islands. An increase of the substrate temperature from 480 to 520°C at optimal arsenic pressure results in an increase of the lateral size of the dot to $\sim 180 \text{ \AA}$ and in a strong decrease of dot density (down to $\sim 1.5-2 \cdot 10^{10} \text{ cm}^{-2}$). The dot lateral shape (well-defined square) is not affected. Large clusters appear locally. The PL peak position shifts slightly ($\sim 30-50 \text{ meV}$) towards higher energy with respect to the PL line for 480°C growth, indicating that the increase of the lateral size is compensated by the reduction of the dot height and the facet angle. Since the stability of the equilibrium dot array strongly depends on the facet surface energy this result is expected because changes in growth parameters influence the surface energy of the InAs layer. MBE growth at optimal conditions is a near-equilibrium process [21]. However, kinetics plays an important role when the process is not equilibrium, and results in macroscopic surface structures ($\sim 1000 \text{ \AA}$) under both low and high arsenic pressures.

In conclusion, self-organisation phenomena are promising for the fabrication of nanostructures in semiconductor epitaxial systems for optoelectronics applications. TEM and HREM appear to be key techniques for structural characterization of nano-objects.

This study was supported by the Office of Energy Research, U.S. Department of Energy under Contract N DE-AC03-76F00098. The use of the facilities of the National Center of Electron Microscopy is greatly appreciated.

References

- [1] L. Goldstein, F. Glas, J.Y. Marzin, M.N. Chavasse, J. Le Roux. Appl. Phys. Lett. **47**, 1099 (1985).
- [2] Y.-W. Mo, D.E. Savage, B.S. Swartzentruber, M.G. Lagally. Phys. Rev. Lett. **65**, 1020 (1990).
- [3] J. Tersoff, R.M. Tromp. Phys. Rev. Lett. **70**, 2782 (1993).
- [4] D. Leonard, M. Krishnamurthy, C.M. Reaves, S.P. Denbaars, P.M. Petroff. Appl. Phys. Lett. **63**, 3203 (1993).
- [5] J.M. Moison, F. Houzay, F. Barthe, L. Leprince, E. Andre, O. Vatel. Appl. Phys. Lett. **64**, 196 (1994).
- [6] N.N. Ledentsov, M. Grundmann, N. Kirstaedter, J. Christen et al. Proc. 22nd Int. Conf. Phys. Sem. Vancouver, Canada (1994). V. 3. P. 1855.
- [7] S. Ruvimov, P. Werner, K. Scheerschmidt, U. Richter et al. Phys. Rev. **B51**, 14 766 (1995).
- [8] R. Nötzel, J. Temmyo, T. Tamamura. Nature **369**, 131 (1994).
- [9] V. Bressler-Hill, A. Lorke, S. Varma, P.M. Petroff, W.H. Weinberg. Phys. Rev. **B50**, 8479 (1994).
- [10] P.D. Wang, N.N. Ledentsov, C.M. Sotomayor Torres, P.S. Kop'ev, V.M. Ustinov. Appl. Phys. Lett. **64**, 1526 (1994).
- [11] E.R. Glawer, B.R. Bennett, V.V. Shanabrook, R. Magno. Appl. Phys. Lett., in press (1997).
- [12] M.C. Harris Liao, H. Chang, Y.F. Chen, J.W. Hsu, J.M. Lin, W.C. Chen. Appl. Phys. Lett. **70**, 2256 (1997).
- [13] F. Glas, C. Gors, P. Henoc. Phil. Mag. **B62**, 373 (1990).
- [14] L.H. Kuo, L.H. Salmanka-Riba, B.J. Wu, J.M. De Puydt, J.M. Haugen, H. Cheng, S. Juha, M.A. Haase. Appl. Phys. Lett. **65**, 1230 (1994).
- [15] A.-L. Barabasi. Appl. Phys. Lett. **70**, 764 (1997).
- [16] R. Nötzel, N.N. Ledentsov, L. Däweritz, M. Hohenstein, K. Ploog. Phys. Rev. Lett. **67**, 3812 (1991).
- [17] V.I. Marchenko. Sov. Phys. JETP **54**, 605 (1981).
- [18] N.N. Ledentsov, V.A. Shchukin, M. Grundmann, N. Kirstaedter et al. Phys. Rev. **B54**, 8743 (1996).
- [19] S. Ruvimov, K. Scheerschmidt. Phys. Stat. Sol. (a) **150**, 471 (1995).
- [20] V.A. Shchukin, N.N. Ledentsov, P.S. Kop'ev, D. Bimberg. Phys. Rev. Lett. **75**, 2968 (1995).
- [21] J. Tersoff, M.D. Johnson, B.G. Orr. Phys. Rev. Lett. **78**, 282 (1997).